



HAL
open science

Robust Regulation of a Power Flow Controller via Nonlinear Integral Action

Tanguy Simon, Mattia Giaccagli, Jean-François Trégouët, Daniele Astolfi,
Vincent Andrieu, Hervé Morel, Xuefang Lin-Shi

► **To cite this version:**

Tanguy Simon, Mattia Giaccagli, Jean-François Trégouët, Daniele Astolfi, Vincent Andrieu, et al.. Robust Regulation of a Power Flow Controller via Nonlinear Integral Action. IEEE Transactions on Control Systems Technology, 2023, 31 (4), pp.1636 - 1648. 10.1109/TCST.2023.3236474 . hal-03920401

HAL Id: hal-03920401

<https://hal.science/hal-03920401v1>

Submitted on 3 Jan 2023

HAL is a multi-disciplinary open access archive for the deposit and dissemination of scientific research documents, whether they are published or not. The documents may come from teaching and research institutions in France or abroad, or from public or private research centers.

L'archive ouverte pluridisciplinaire **HAL**, est destinée au dépôt et à la diffusion de documents scientifiques de niveau recherche, publiés ou non, émanant des établissements d'enseignement et de recherche français ou étrangers, des laboratoires publics ou privés.

Robust Regulation of a Power Flow Controller via Nonlinear Integral Action

Tanguy Simon, *Student Member, IEEE*, Mattia Giaccagli, *Student Member, IEEE*, Jean-François Trégouët, Daniele Astolfi, *Member, IEEE*, Vincent Andrieu, Hervé Morel, *Senior Member, IEEE* and Xuefang Lin-Shi

Abstract—This paper considers a robust output set-point tracking problem for a m -terminal power flow controller (PFC) for meshed DC micro-grids. The PFC is a power electronics device used to control the power flow at a node in the meshed grid, and may act as a DC circuit breaker. The system is modelled by state-space bilinear dynamics coupled with a polynomial output. In the proposed design, the plant is first extended with an integral action processing the regulation error. The cascaded model composed of the plant and the integrator is then stabilised using a saturated state-feedback law, designed with a forwarding approach. An anti-windup function is added to cope with transient saturations. A tuning method is proposed to set the controller gains along the available degrees of freedom with respect to a cost function. The stability of the closed-loop is guaranteed for any compact set of initial conditions and for small parametric variations around the nominal set-point. Experiments have been carried out and these properties are successfully assessed on a tenth-scale experimental set-up.

Index Terms—Bilinear systems, integral action, meshed micro-grids, power flow controllers, robust control, forwarding

I. INTRODUCTION

In the light of the current climate breakdown, it is of paramount importance to cut global greenhouse gas emissions. The access to electrical energy holds an important place in these discussions, and direct current (DC) micro-grids respond favourably to those issues. This type of electrical power network enhances the penetration of small renewable energy generators and lowers the energy losses, while helping the clean access to electrical energy or the transition to a more energy-frugal lifestyle (see, e.g., [1], [2] and references therein for a broader discussion on the subject). The meshed structure of micro-grids improves this result by reducing the amount of copper needed (because there can be multiple paths between two points and the average power in each line in a building

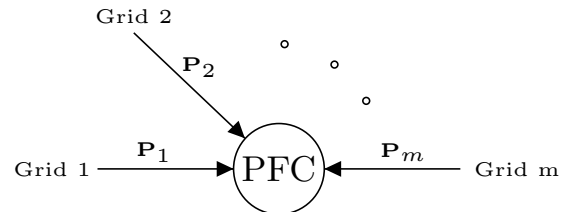


Fig. 1. m -terminal PFC at a node in the grid.

is low), as well as improving the reliability, modularity and efficiency of the system [3].

To control a meshed DC grid, a DC Power Flow Controller (PFC) is required. It is a multi-terminal DC-DC converter located at a node in the mesh, sometimes called a smart-node [4]. Its objective is the regulation of the power in each line of the node (see Fig. 1), despite the high intermittency of renewable generators.

Although PFCs for high voltage DC applications (HVDC) have received a strong academic interest (see, e.g., the recent survey [5]) very little has been done for low-voltage applications (LVDC). The lower voltage rating leads to a completely different converter topology, and therefore to different control schemes. Among them, recall a multi-terminal PFC with a compensation node [6] improved by removing the compensation node [7], a PFC made of two separate Split-PI converters [8], and a three-terminal PFC [2], [9]. The main shortcomings of [6]–[8] are the absence of dynamic model and their control strategies, which fail to give any proof of stability or robustness. No direct control of the power is achieved, and the control laws are applied to two-terminal devices, which do not constitute a node. In [6], the control law is a constant ratio determined by a look-up table, based on the knowledge of the voltage at the end of the line, an uncertain parameter in practice. In [7], a PI controller is used to regulate the current instead of the power, whose reference is again computed using the voltage at the end of the line. Moreover, the reservoir voltage, which is the voltage on a capacitor inside the converter, is not controlled and can drift outside the physical boundaries. Finally, in [8], the authors propose a current-limited voltage controller using the RST technique with hysteresis switching. The reservoir voltage is properly controlled but power flow control is not achieved.

In this study, a m -terminal power flow controller is considered. Assume a synchronous PWM switching scheme on each branch, and suppose that the grid's dynamics are partially

T.Simon, J-F.Trégouët, H.Morel and X.Lin-Shi are with Univ Lyon, INSA Lyon, Université Claude Bernard Lyon 1, Ecole Centrale de Lyon, CNRS, AMPERE, F-696 21, Lyon, France. Emails: tanguy.simon@insa-lyon.fr, jean-francois.tregouet@insa-lyon.fr, herve.morel@insa-lyon.fr, xuefang.shi@insa-lyon.fr

M.Giaccagli, D. Astolfi and V. Andrieu are with Université Claude Bernard Lyon 1, CNRS, LAGEPP UMR 5007, 43 boulevard du 11 novembre 1918, F-69100, Villeurbanne, France. Emails: mattia.giaccagli@univ-lyon1.fr, daniele.astolfi@univ-lyon1.fr, vincent.andrieu@univ-lyon1.fr

unknown to take into account its high variability. In this context, the PFC in the grid has been recently modeled using a state-space approach [2]. The resulting continuous-time and finite-dimensional model is uncertain and bilinear. Moreover, the output to be regulated is a second-order polynomial. Indeed, this signal corresponds to the electrical power in all the lines, and this quantity is the product of couples of state variables, i.e. the voltage and current in each line.

The corresponding control problem is challenging as it is associated with a system which is non-linear, uncertain and with a non-linear output. While many papers dealing with stabilisation problems for bilinear systems can be found in the literature (see, for instance, [10]–[16]), very few addressed the more general problem of output regulation, e.g., [17], and more recently [18], [19], and all of them are focused on control designs for systems having a pure linear output and are therefore not directly applicable to the problem explained above. Despite this lack of literature on output regulation, bilinear systems are a class of systems commonly employed to model physical systems, such as a heat exchanger [20], hydraulic systems [21], power factor compensators and HVDC converters [18], microbial cell growth [22] and many others [23].

Nevertheless, direct power flow control is achieved in [2] on a three-terminal PFC, using a state feedback on the linearised dynamics after adding integrators. Yet, this first attempt only gives local stability results in the state-space, and although its robustness has been tested, no proofs are given for local stability in the parametric space. Furthermore, the saturation of the duty cycles is not taken into account when designing the controller.

The authors' contributions with respect to the literature are the following. (i) The proposed controller achieves semi-global asymptotic stability in the state-space and provides robustness with respect to small parameter variations. To this end, model uncertainties and non-linearities are directly taken into account at the design step. In a nutshell, the PFC model is first extended with an integral action processing the regulation error. Then, a stabiliser for the extended system is derived following the so-called “forwarding approach” (see, e.g., [24]–[26] or [27]–[29] for an incremental version). This control law inherits stability properties with respect to small parameter variations as shown in [25], [30]. (ii) An arbitrary number of terminals is considered, i.e. $m \geq 2$ can be any integer. (iii) As the control inputs are physically represented by the duty cycles of each terminal, a saturation is applied to the control action to meet such constraints. Comparing to the unconstrained case, the closed-loop basin of attraction is preserved through the implementation of an anti-windup correction term to deal with (possible) unstable behaviours of the integrator dynamics with such input saturation. (iv) A tuning procedure for the controller gains is offered. (v) All these achievements are successfully assessed on a real tenth-scale test-bench for $m = 3$, and via simulations for a larger number of terminals.

A preliminary conference version of this paper was presented in [9]. Here, as compared with [9], 1) a controller for the m -terminal PFC is proposed to improve the applicability of the proposed method, whereas [9] is concerned with the

TABLE I
Symbols

Electrical			
C_f	Filter capacitance	C_R	Reservoir capacitance
\mathbf{i}_k, i_k	Current in L_f	\mathbf{i}_{Gk}, i_{Gk}	Grid current
L_f	Filter inductance	L_{Gk}	Grid inductance
P_k	Power in line k	R_{Gk}	Grid resistance
\mathbf{v}_k, v_k	Line voltage (on C_f)	V_{Gk}	Grid voltage
\mathbf{v}_R, v_R	Reserv. volt. (on C_R)		
State-space			
\mathbf{A}, A	Dynamic matrix	B	Input matrix
\mathbf{C}, C	Output matrix	\mathbf{H}, H	Polynomial out. mat.
\mathbf{J}	“Inertia” matrix	\mathbf{N}, N	Bilinear input mat.
\mathbf{q}	Constant vector	\mathbf{r}	Reference vector
\mathbf{u}, u	Input vector	\mathbf{w}, w	Aug. state vector
\mathbf{x}, x	State vector	\mathbf{y}, y	Output vector
\mathbf{z}, z	Integrator vector	δ	Set-point vector
θ	Parameter vector	$\varphi(\cdot)$	aug. cl.-loop dynamics
n	number of states	m	number of inputs
p	number of outputs	n_z	number of integrators
ξ	integral action	α, ψ	control laws
ζ	anti windup	P, Ω, M	control actions
d, \underline{d}	A.W. tuning		
Sets			
\mathcal{D}	Possible set-points	$\mathcal{E}(\delta)$	Equilibrium points
\mathcal{R}	Possible references	\mathcal{S}	Admissible set-points
\mathcal{U}	Admissible inputs	Θ	Possible parameters
Accents, indexes and exponents			
\sim	see Section IV-C	r	Reference
*	Equilibrium	$_{\text{nom}}$	On nominal set-point
bold	absolute coordinates	<i>slim</i>	error coordinates

particular case of $m = 3$; 2) The saturation of the duty cycles is taken into account, not only in the simulation but also in the theoretical proofs, and an anti-windup design is proposed; 3) Additional degrees of freedom are provided in the control design, and a tuning procedure is proposed; 4) All these extensions have been successfully implemented on a real tenth-scale test-bench for $m = 3$ and via simulations for a larger number of terminals, while in [9] only simulations on a 3-terminal PFC have been implemented to validate the proposed control design.

The paper is organised as follows. In Section II, the model of the power flow controller is presented and the studied control problem is formalised. In Section III, the forwarding control approach is reviewed and specialised to the case of bilinear systems having a second-order polynomial output. Section IV contains the main theoretical results of the paper. The control law design is presented and it is shown that such a design guarantees global asymptotic stability of the nominal equilibrium of the closed-loop system. Such design is proven to be (locally) robust, i.e. it ensures that the regulation is achieved even in the case of sufficiently small parameter uncertainties. Finally, a tuning procedure is proposed for the control law. In Section V, the experimental measurements are presented on a 3-terminal PFC, along with simulations on a 5-terminal one. Finally, conclusions are given in Section VI. Proofs of technical Lemmas are postponed to the Appendix.

Notation. The operator “diag { }” builds a diagonal matrix

from entries of the input vector argument. Given a vector $a \in \mathbb{R}^n$, the notation a_k refers to the k -th element of a , with 1 being the index of the first element. The symbol \mathbf{I}_m stands for the identity matrix of size $m \times m$ and $\mathbf{1}_m$ for the column vector of size m in which each element is 1. The null matrix of size $m \times n$ is denoted by $\mathbf{0}_{m \times n}$ while $\mathbf{0}_m$ denotes column vectors. Dimensions are omitted when obvious from the context. Note $\llbracket 1, m \rrbracket$ as every integer between 1 and m included, i.e. $\llbracket 1, m \rrbracket = \{1, \dots, m\}$. Given a square matrix A , $\det(A)$ indicates its determinant. Given a set \mathcal{S} , $\text{card}(\mathcal{S})$ denotes its cardinality and $\text{int}(\mathcal{S})$ its interior. Given a set $[a_1, a_2] \subset \mathbb{R}$, the notation $[a_1, a_2]^n$ denotes the set $[a_1, a_2]^n := [a_1, a_2] \times \dots \times [a_1, a_2] \subset \mathbb{R}^n$. Define the following asymmetrical scalar saturation function $\text{sat}_{\underline{s}}^{\bar{s}}: \mathbb{R} \rightarrow \mathbb{R}$ as

$$\text{sat}_{\underline{s}}^{\bar{s}}(s) = \begin{cases} \underline{s} & \text{if } s < \underline{s} \\ s & \text{if } \underline{s} \leq s \leq \bar{s} \\ \bar{s} & \text{if } s > \bar{s} \end{cases}$$

for some constants $\underline{s} \leq \bar{s} \in \mathbb{R}$ and the following scalar dead-zone function $\text{dz}_d: \mathbb{R} \rightarrow \mathbb{R}$ as

$$\text{dz}_d(s) = s - \text{sat}_{-d}^d(s)$$

for some constant $d > 0$. Then, given any two vectors $\bar{s} = [\bar{s}_1 \ \dots \ \bar{s}_m]^\top \in \mathbb{R}^m$, $\underline{s} = [\underline{s}_1 \ \dots \ \underline{s}_m]^\top \in \mathbb{R}^m$ and any scalar $d \in \mathbb{R}$, define the following (vector) saturation function $\text{Sat}_{\underline{s}}^{\bar{s}}: \mathbb{R}^m \rightarrow \mathbb{R}^m$ and the following (vector) dead-zone function $\text{Dz}_d: \mathbb{R}^m \rightarrow \mathbb{R}^m$ as

$$\text{Sat}_{\underline{s}}^{\bar{s}}(s) = \begin{bmatrix} \text{sat}_{\underline{s}_1}^{\bar{s}_1}(s_1) \\ \vdots \\ \text{sat}_{\underline{s}_m}^{\bar{s}_m}(s_m) \end{bmatrix}, \quad \text{Dz}_d(s) = \begin{bmatrix} \text{dz}_d(s_1) \\ \vdots \\ \text{dz}_d(s_m) \end{bmatrix}, \quad (1)$$

for some vector $s = [s_1 \ \dots \ s_m]^\top \in \mathbb{R}^m$, i.e. as the functions that implement element-wise, respectively, the sat and dz function defined before. Note that the saturation constants in $\text{Sat}_{\underline{s}}^{\bar{s}}$ are different element-wise. A summary of the notation used in this article is given in Table I to aid the reader.

II. PROBLEM STATEMENT

The Power Flow Controller (PFC) is an electrical device whose objective is to control the electric power in the lines it is connected to. As shown in Fig. 1, in this article, a general m -terminal version is considered. The chosen electrical circuit to achieve this function is made of m identical buck-boost converters whose high-side are connected in parallel to a unique reservoir capacitor noted C_R . Each branch (buck-boost) is depicted on the left of Fig. 2. The grid connected to terminal k , as seen by the PFC, is modelled by a Thevenin equivalent circuit, as drawn on the right-hand side of the same figure. This equivalent circuit aims at capturing the dynamics of the network, originating from the interplay between the impedance of the conductors and the dynamics of the loads/generators connected to the grid.

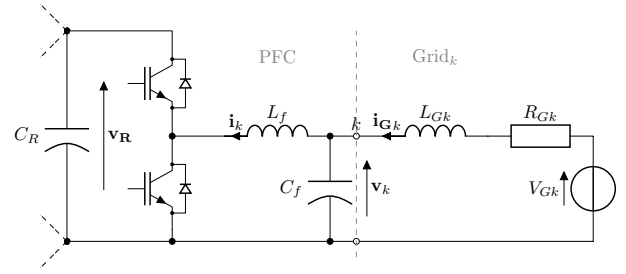


Fig. 2. Detail of the k -th branch of the PFC (left) and the Thevenin grid model as seen by this terminal (right)

This circuit cannot operate properly if the reservoir voltage is not controlled¹. This adds another control objective which can be solved knowing that such a voltage is constant if and only if the sum of average powers is equal to zero. Consequently, if the reservoir voltage is regulated to a constant value v_R^r and all the lines but one are regulated to a constant power reference P_k^r for $k \in \llbracket 1, m-1 \rrbracket$, the power in the last line naturally converges to the overall power balance, i.e. P_m^r tends to $-\sum_{k=1}^{m-1} P_k^r$.

The problem tackled in this paper is the following: design a state-feedback controller delivering the duty ratios for the pulse-width modulation (PWM) switching of the transistors to achieve power control in each line of the node, while maintaining the reservoir voltage to a fixed given constant value, despite the uncertainty of the parameters characterising the grid. Moreover, to ensure flexibility and modularity, assume limited knowledge on the grid model at the end of each line.

A. Model of The Power Flow Controller

In Fig. 2, the currents are denoted by i and measured in Amps and the dynamic voltages by v and measured in Volts. Note that the line voltage should be positive in a grid (more specifically within a precise tolerance of the nominal voltage), therefore every steady-state voltage v_k^* will be considered non-negative. The component parameters are denoted by L_f/L_{Gk} , C_f/C_R , R_{Gk} and V_{Gk} for, respectively, inductors (Henry), capacitors (Farad), resistors (Ohm) and constant voltages (Volts). The dynamic model of the system can be derived by using Kirchhoff's and Ohm's electrical laws, along with the dynamic electrical laws for inductors and capacitors, while assuming ideal components, see, [2] for a more detailed construction of the PFC's model. A synchronous PWM switching is implemented, and the dynamics are averaged over a switching period. The input vector $\mathbf{u} = [u_1, \dots, u_m]^\top \in \mathbb{R}^m$ is made of the duty ratio of each terminal and hence each of the $u_i(t)$ must be included in the set $[0, 1] \subset \mathbb{R}$ for all $t \geq 0$. Therefore, the set of admissible inputs is defined as

$$\mathcal{U} := [0, 1]^m \quad (2)$$

The dynamic variables are all gathered in the state vector $\mathbf{x} \in \mathbb{R}^n$ with $n = 3m + 1$, and the uncertain model parameters are collected in the vector $\theta \in \mathbb{R}^{3m}$, as shown in Table II.

¹If $v_R < v_k$ for some $k \in \llbracket 1, m \rrbracket$, the current flows freely through the diode in the upper transistor of the k^{th} branch, which cannot be controlled by the PWM switching (see Fig. 2)

The output vector corresponds to the control objectives $\mathbf{y} = [\mathbf{P}_1, \dots, \mathbf{P}_{m-1}, \mathbf{v}_R]^\top \in \mathbb{R}^m$, with $\mathbf{P}_k = \mathbf{i}_{Gk} \mathbf{v}_k$. A state-space model can then be obtained for the PFC, following the results in [2]. The system can be represented as a bilinear system. The states are the currents $\mathbf{i}_k, \mathbf{i}_{Gk}$ and the voltages \mathbf{v}_k for $k \in \llbracket 1, m \rrbracket$ and \mathbf{v}_R . Additionally, the PFC is coupled with a polynomial output on which the regulation task has to be achieved. Such an output is composed by the powers \mathbf{P}_k for $k \in \llbracket 1, m \rrbracket$ and the reservoir voltage \mathbf{v}_R . In details, it can be described by a set of dynamical equations of the form

$$\begin{aligned} \dot{\mathbf{x}} &= \mathbf{A}(\theta)\mathbf{x} + \mathbf{N}(\mathbf{x})\mathbf{u} + \mathbf{q}(\theta), \\ \mathbf{y} &= \mathbf{C}\mathbf{x} + \mathbf{H}(\mathbf{x})\mathbf{x}, \\ \mathbf{u} &\in \mathcal{U}, \end{aligned} \quad (3)$$

with

$$\mathbf{A}(\theta) = \mathbf{J}(\theta)^{-1} \begin{bmatrix} 0 & \mathbf{0}_m^\top & \mathbf{0}_m^\top & \mathbf{0}_m^\top \\ \mathbf{0}_m & \mathbf{0} & \mathbf{I}_m & \mathbf{0} \\ \mathbf{0}_m & -\mathbf{I}_m & \mathbf{0} & \mathbf{I}_m \\ \mathbf{0}_m & \mathbf{0} & -\mathbf{I}_m & -\text{diag}\{R_G\} \end{bmatrix} \quad (4a)$$

$$\mathbf{N}(\mathbf{x})\mathbf{u} = \sum_{j=1}^m (\mathbf{N}_j \mathbf{u}_j) \mathbf{x} = \mathbf{J}(\theta)^{-1} \begin{bmatrix} 0 & \mathbf{u}^\top & \mathbf{0}_{2m}^\top \\ -\mathbf{u} & \mathbf{0} & \mathbf{0} \\ \mathbf{0}_{2m} & \mathbf{0} & \mathbf{0} \end{bmatrix} \mathbf{x}, \quad (4b)$$

$$\mathbf{q}(\theta) = \mathbf{J}(\theta)^{-1} [\mathbf{0}_{n-m}^\top, V_G^\top]^\top, \quad (4c)$$

$$\mathbf{J}(\theta) = \text{diag}\{C_R, \mathbf{1}_m^\top L_f, \mathbf{1}_m^\top C_f, L_G^\top\}, \quad (4d)$$

$$\mathbf{C} = \begin{bmatrix} \mathbf{0}_{m-1} & \mathbf{0} \\ 1 & \mathbf{0}_{n-1}^\top \end{bmatrix}, \quad (4e)$$

$$\mathbf{H}(\mathbf{x}) = \begin{bmatrix} \mathbf{0} & \frac{1}{2} \text{diag}\{\mathbf{i}_{G1}, \dots, \mathbf{i}_{Gm-1}\} & \mathbf{0}_{m-1} \\ \mathbf{0}_{1+m}^\top & \mathbf{0}_{m-1}^\top & 0 \\ & \frac{1}{2} \text{diag}\{\mathbf{v}_1, \dots, \mathbf{v}_{m-1}\} & \mathbf{0}_{m-1} \\ & \mathbf{0}_{m-1}^\top & 0 \end{bmatrix} \quad (4f)$$

where, for each $j = 1, \dots, m$, the \mathbf{N}_j are constant $n \times n$ matrices defined as $\mathbf{N}_j = \mathbf{J}(\theta)^{-1} N_j$ where N_j are m different matrices full of zeros with a 1 in the first row and $j + 1$ column and a -1 in the first column and $j + 1$ row, and with $L_G = [L_{G1}, \dots, L_{Gm}]$, $R_G = [R_{G1}, \dots, R_{Gm}]$ and $V_G = [V_{G1}, \dots, V_{Gm}]$. Let $\Theta \subset \mathbb{R}^{3m}$ be the non-empty set of possible system parameters that are compatible with the physics of the system. It is defined as

$$\Theta := \left\{ \theta \in \mathbb{R}^{3m} : L_{Gk} > 0, R_{Gk} > 0, V_{Gk} \geq 0, k \in \llbracket 1, m \rrbracket \right\}. \quad (5)$$

There is no loss of generality in these constraints since L_G, R_G represent physical properties (inductance and resistance) which are always strictly positive. As shown later in (42a), $\mathbf{P}_k^r = 0$ implies $\lim_{t \rightarrow +\infty} \mathbf{v}_k(t) = \mathbf{v}_k^* = V_{Gk}$, i.e. when the power reference is null, the line voltage tends to V_{Gk} . As stated before, this line voltage should always be non-negative, then so should V_{Gk} .

The vector of references corresponds to the control objectives, i.e. $\mathbf{r} = [\mathbf{P}_1^r, \dots, \mathbf{P}_{m-1}^r, \mathbf{v}_R^r]^\top$, and the non-empty set

TABLE II
State vector and uncertain parameter vector.

\mathbf{x}	\mathbf{x}_1	\mathbf{x}_2	\dots	\mathbf{x}_{m+1}	\mathbf{x}_{m+2}	\dots	\mathbf{x}_{2m+1}	\mathbf{x}_{2m+2}	\dots	\mathbf{x}_{3m+1}
\mathbf{v}_R	\mathbf{i}_1	\dots	\mathbf{i}_m	\mathbf{v}_1	\dots	\mathbf{v}_m	\mathbf{i}_{G1}	\dots	\mathbf{i}_{Gm}	
θ	θ_1	\dots	θ_m	θ_{m+1}	\dots	θ_{2m}	θ_{2m+1}	\dots	θ_{3m}	
	L_{G1}	\dots	L_{Gm}	R_{G1}	\dots	R_{Gm}	V_{G1}	\dots	V_{Gm}	

of possible references $\mathcal{R} \subseteq \mathbb{R}^m$ is defined as

$$\mathcal{R} := \left\{ \mathbf{r} = (\mathbf{P}_1^r, \dots, \mathbf{P}_{m-1}^r, \mathbf{v}_R^r) \in \mathbb{R}^m : (\mathbf{P}_1^r, \dots, \mathbf{P}_{m-1}^r) \neq (0, \dots, 0), \mathbf{v}_R^r > 0 \right\}. \quad (6)$$

where, as stated before, \mathbf{v}_R^r should be sufficiently high for the device to operate properly and hence only strictly positive values have been taken into consideration. The case in which all the reference powers \mathbf{P}_j^r are null has not been taken into consideration, as it makes the control objective structurally impossible, as shown later on.

B. Control problem

This article focuses on a robust regulation problem for the PFC represented by the model (3). Define beforehand the compact notation $\delta := (\theta, \mathbf{r})$ and $\mathcal{D} := \Theta \times \mathcal{R}$. The tackled problem is stated as follows.

Problem. Given a nominal set of parameters \mathcal{D} and $\delta_{\text{nom}} \in \mathcal{D}$, find functions $\xi : \mathbb{R}^n \times \mathbb{R}^{n_z} \rightarrow \mathbb{R}^{n_z}$ and $\alpha : \mathbb{R}^n \times \mathbb{R}^{n_z} \rightarrow \mathcal{U}$ such that for any arbitrarily large compact set of initial conditions $\mathcal{X} \times \mathcal{Z} \subseteq \mathbb{R}^n \times \mathbb{R}^{n_z}$ there exists $\bar{\delta} > 0$ such that, for any δ satisfying $\|\delta - \delta_{\text{nom}}\| \leq \bar{\delta}$, the resulting trajectories of system (3) in closed-loop with the regulator

$$\begin{aligned} \dot{\mathbf{z}} &= \xi(\mathbf{x}, \mathbf{z}), \\ \mathbf{u} &= \alpha(\mathbf{x}, \mathbf{z}) \end{aligned}$$

are bounded forward in time and $\lim_{t \rightarrow \infty} \mathbf{y}(t) = \mathbf{r}$.

Following an *internal model* based design (see, e.g., [25], [31]), the system (3) is first extended with an integral action processing the regulation error as follows

$$\dot{\mathbf{z}} = \mathbf{y} - \mathbf{r}. \quad (7)$$

Indeed, as shown in [25], the use of the integral action (7) is necessary to achieve asymptotic tracking in the presence of (sufficiently small) perturbations of the plant model in every direction. The key feature of the integral action is that if there exists an equilibrium for the closed-loop system, then the regulation error is necessarily equal to 0 at this equilibrium. Furthermore, the control law is saturated since $\mathbf{u} \in \mathcal{U}$, and this physical constraint may lead to unstable behaviours in the dynamics of the integrator. To deal with this issue, an anti-windup design is implemented (see [32]–[34]) to mitigate the effects of uncontrollable integral action. This leads to the following integral dynamics

$$\dot{\mathbf{z}} = \xi(\mathbf{x}, \mathbf{z}) := \mathbf{y} - \mathbf{r} + \zeta(\mathbf{x}, \mathbf{z}) \quad (8)$$

where the function ζ represents such an anti-windup. The overall proposed control scheme is depicted in Fig. 3. The

design of the function $\alpha(\cdot)$ that has been implemented, follows the so-called forwarding approach. The next section specialises and enriches such a technique to the class of bilinear systems having a second-order polynomial output.

III. FORWARDING DESIGN FOR A CLASS OF BILINEAR SYSTEMS WITH A POLYNOMIAL OUTPUT

Consider a system composed by a cascade of a bilinear system having a second-order polynomial output feeding an integrator of the form

$$\begin{aligned}\dot{x} &= Ax + (N(x) + B)u, \\ \dot{z} &= Cx + H(x)x,\end{aligned}\quad (9)$$

where $(x, z) \in \mathbb{R}^{n+p}$ is the state, $u \in \mathbb{R}^m$ is the control input, A, B, C are matrices of suitable dimensions, and functions $H: \mathbb{R}^n \rightarrow \mathbb{R}^{p \times n}$ and $N: \mathbb{R}^n \rightarrow \mathbb{R}^{n \times m}$ defined as $H(x) = [H_1^\top x \ \dots \ H_p^\top x]^\top$ and $N(x) = [N_1 x \ \dots \ N_m x]$ for some $n \times n$ matrices $H_1, \dots, H_p, N_1, \dots, N_m$.

Standing Assumption. *The number of inputs is not smaller than the number of outputs, i.e. $m \geq p$.*

The following result specialises the forwarding control design (see, e.g., [25]–[28], [30] and the references therein) for systems of the form of (9).

Proposition 1. *Consider system (9). Suppose that A is Hurwitz and that the matrix $CA^{-1}B$ is full rank. Select $P = P^\top \succ 0$ and $M_i = M_i^\top$ such that*

$$PA + A^\top P \prec 0, \quad (10)$$

$$M_i A + A^\top M_i = \frac{1}{2}(H_i + H_i^\top), \quad \forall i \in \llbracket 1, p \rrbracket, \quad (11)$$

and let $M_0 = CA^{-1}$. Then, for any matrix $\Omega = \Omega^\top \succ 0$, the origin of system (9) in closed-loop with $u = \psi(x, z)$, with the function $\psi: \mathbb{R}^{n+p} \rightarrow \mathbb{R}^m$ defined as

$$\begin{aligned}\psi(x, z) &= -\left(x^\top P(N(x) + B) \right. \\ &\quad \left. - (z - M(x))^\top \Omega (M_0 + 2R(x))(N(x) + B)\right)^\top,\end{aligned}\quad (12)$$

with

$$R(x) := [M_1 x \ \dots \ M_p x]^\top \quad (13)$$

$$M(x) := M_0 x + R(x)x, \quad (14)$$

is globally asymptotically stable and locally exponentially stable.

Proof. The proof is based on a Lyapunov function construction which follows the results presented in [26]. In particular, let $W: \mathbb{R}^{n+p} \rightarrow \mathbb{R}$ be defined as

$$W(x, z) = \frac{1}{2}x^\top P x + \frac{1}{2}(z - M(x))^\top \Omega (z - M(x)), \quad (15)$$

with P and M defined respectively by (10) and (14) as in the statement of the proposition. Note that W is proper and

positive definite. By construction, the function M satisfies

$$\begin{aligned}\frac{\partial M}{\partial x}(x)Ax &= M_0 Ax + \begin{bmatrix} x^\top (M_1 A + A^\top M_1)x \\ \vdots \\ x^\top (M_p A + A^\top M_p)x \end{bmatrix}, \\ &= Cx + \frac{1}{2} \begin{bmatrix} x^\top (H_1 + H_1^\top)x \\ \vdots \\ x^\top (H_p + H_p^\top)x \end{bmatrix} \\ &= Cx + H(x)x.\end{aligned}\quad (16)$$

Hence, the time derivative of W along the solutions of system (9) satisfies

$$\begin{aligned}\dot{W}(x, z) &= x^\top (PA + A^\top P)x + [x^\top P(N(x) + B) \\ &\quad - (z - M(x))^\top \Omega (M_0 + 2R(x))(N(x) + B)]u,\end{aligned}$$

where the relation (16) has been used. Using again the definition of M in (14) and the definition of ψ in (12) yields

$$\dot{W}(x, z) = x^\top (PA + A^\top P)x - \psi^\top(x, z)\psi(x, z) \leq 0.$$

Furthermore, note that

$$\{(x, z) : \dot{W}(x, z) = 0\} = \{(x, z) : x = 0, \psi(x, z) = 0\}.\quad (17)$$

Moreover, using the definition of M_0 , $\psi^\top(0, z) = z^\top \Omega C A^{-1} B$ is obtained. Since by assumption, $CA^{-1}B$ and Ω are full rank, the set $\{(x, z) : \dot{W}(x, z) = 0\}$ coincides with the origin and therefore $(x, z) \mapsto \dot{W}(x, z)$ is negative definite. Consequently, W is a Lyapunov function of the closed-loop system and the origin is globally asymptotically stable. Finally, employing the same method, note that the quadratic function

$$W_0(x, z) = \frac{1}{2}x^\top P x + \frac{1}{2}(z - M_0 x)^\top \Omega (z - M_0 x),$$

is a Lyapunov function for the first-order approximation

$$\dot{x} = Ax + B\psi_0(x, z), \quad \dot{z} = Cx,$$

with $\psi_0(x, z)$ being the first-order approximation of ψ . Hence, local exponential stability of the equilibrium is obtained. \square

IV. MAIN RESULTS

In this section, the main theoretical results of the paper are stated. Given the PFC model (3), a first detailed analysis of the set of solutions that solve the problem is given. Then, the controller design shown in Fig. 3 is presented. It is defined as an integral action processing the tracking error implemented with an anti-windup design, and a state-feedback stabiliser for the closed-loop based on forwarding design. It will also be shown that the presented design is able to achieve output regulation even in the case of (sufficiently small) parameter uncertainties. Moreover, a tuning procedure for the control gains is provided.

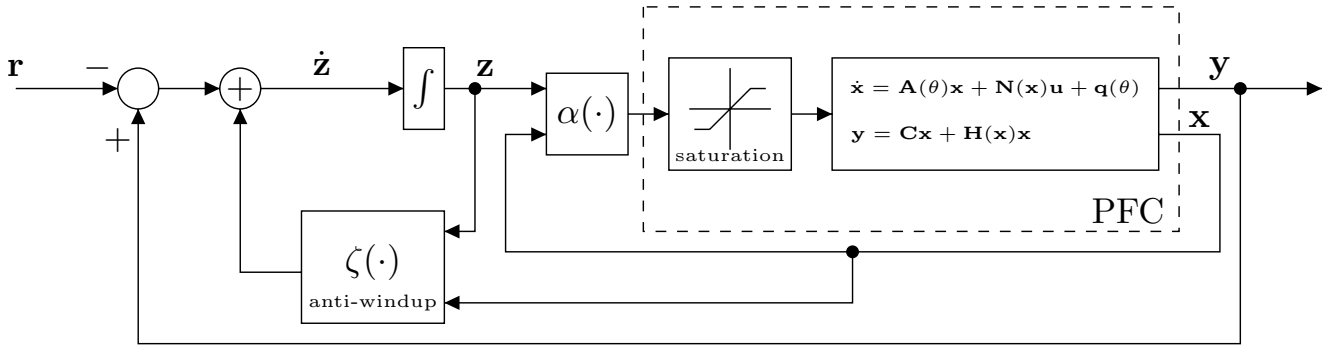


Fig. 3. Proposed control structure for the PFC

A. Set of solutions

The considered problem may not be solvable for all $\delta = (\theta, \mathbf{r}) \in \mathcal{D}$ since for some values of δ there may not exist an equilibrium pair $(\mathbf{x}^*, \mathbf{u}^*)$ satisfying $\mathbf{y} = \mathbf{r}$ within the input constraints. Therefore, for a given $\delta \in \mathcal{D}$, let $\mathcal{E}(\delta)$ be the set of admissible equilibrium points, namely the set of steady-state solutions on which output regulation is achieved, i.e.

$$\mathcal{E}(\delta) := \left\{ (\mathbf{x}^*, \mathbf{u}^*) \in \mathbb{R}^n \times \mathcal{U} : \mathbf{A}(\theta)\mathbf{x}^* + \mathbf{N}(\mathbf{x}^*)\mathbf{u}^* + \mathbf{q}(\theta) = 0, \mathbf{C}\mathbf{x}^* + \mathbf{H}(\mathbf{x}^*)\mathbf{x}^* = \mathbf{r} \right\}. \quad (18)$$

The set \mathcal{S} is then defined as the set of admissible parameters and references δ for which there exists such equilibrium points:

$$\mathcal{S} := \{ \delta \in \mathcal{D} : \text{card}(\mathcal{E}(\delta)) > 0 \}. \quad (19)$$

A characterisation of \mathcal{S} can then be provided through model inversion as shown below, whose proof has been postponed to the appendix.

Proposition 2. Consider system (3). Then

$$\mathcal{S} = \left\{ \delta \in \mathcal{D} : \Delta_k(\delta) \geq 0, 0 \leq \frac{1}{2\mathbf{v}_{\mathbf{R}^r}} \left(V_{Gk} \pm \sqrt{\Delta_k(\delta)} \right) \leq 1, k \in \llbracket 1, m \rrbracket \right\}, \quad (20)$$

where

$$\Delta_k(\delta) := V_{Gk}^2 - 4R_{Gk}\mathbf{P}_k^r \quad (21)$$

with $\mathbf{P}_m^r := -\sum_{k=1}^{m-1} \mathbf{P}_k^r$. Moreover, for a given $\delta \in \mathcal{S}$, there exists from one to 2^m pairs $(\mathbf{x}^*, \mathbf{u}^*) \in \mathcal{E}(\delta)$.

B. Controller design

This section aims to solve the regulation problem presented in Section II-B for the PFC (3) following the control structure presented in Fig. 3. The controller is designed for some known nominal parameters and references $\delta_{\text{nom}} := (\theta_{\text{nom}}, \mathbf{r}_{\text{nom}})$. Furthermore, it is assumed that this pair belongs to $\text{int}(\mathcal{S})$. This allows to prove that output set-point tracking is still achieved for δ distinct from δ_{nom} but sufficiently close to it, as specified later on. The main result of the paper is stated as follows.

Theorem 1. Consider the set \mathcal{S} defined in (19). Select any $\delta_{\text{nom}} = (\theta_{\text{nom}}, \mathbf{r}_{\text{nom}}) \in \text{int}(\mathcal{S})$ and any corresponding

$(\mathbf{x}_{\text{nom}}^*, \mathbf{u}_{\text{nom}}^*) \in \mathcal{E}(\delta_{\text{nom}})$. Then, for $d > 0$ sufficiently high, the Problem for system (3) is solved by the control law

$$\begin{aligned} \dot{\mathbf{z}} &= \xi(\mathbf{x}, \mathbf{z}) := \mathbf{y} - \mathbf{r} - \text{Dz}_d(\mathbf{z} - M(\mathbf{x} - \mathbf{x}_{\text{nom}}^*)) \\ \mathbf{u} &= \alpha(\mathbf{x}, \mathbf{z}) := \mathbf{u}_{\text{nom}}^* + \text{Sat}_{-\mathbf{u}_{\text{nom}}^*}^{1-\mathbf{u}_{\text{nom}}^*}(\psi(\mathbf{x} - \mathbf{x}_{\text{nom}}^*, \mathbf{z})) \end{aligned} \quad (22)$$

where the functions Sat and Dz are defined in (1), the function ψ is chosen as (12) with the matrices A, B, C and functions N, H defined as

$$\begin{aligned} A &:= \mathbf{A}(\theta_{\text{nom}}) + \sum_{j=1}^m \mathbf{N}_j \mathbf{u}_{\text{nom},j}^*, & B &:= \mathbf{N}(\mathbf{x}_{\text{nom}}^*) \\ C &:= \mathbf{C} + 2\mathbf{H}(\mathbf{x}_{\text{nom}}^*), & N(x) &:= \mathbf{N}(x), \end{aligned}$$

$H(x) := \mathbf{H}(x)$, P, M defined as in (10), (14) and any $\Omega = \Omega^T \succ 0$.

Remark 1. Note that the integral action dynamics is designed in the form of (8) with the anti-windup term that takes the form of a dead-zone function. The function α is selected as a first (nominal) feed-forward action $\mathbf{u}_{\text{nom}}^*$ plus a second term made by saturating the function ψ derived from the forwarding approach in Proposition 1. Thanks to the saturation, the stabiliser satisfies the input constraints as α takes only values in \mathcal{U} , ensuring the validity of the control law with respect to the model (3). Indeed the following holds

$$0 \leq \mathbf{u} = \mathbf{u}_{\text{nom}}^* + \text{Sat}_{-\mathbf{u}_{\text{nom}}^*}^{1-\mathbf{u}_{\text{nom}}^*}(\psi(x, z)) \leq 1$$

In this sense, note that the control law ψ in Proposition 1 is of infinite gain margin, i.e. $\kappa\psi(\cdot)$ is still a stabiliser for (9) for all gains $\kappa > 0$, and hence the saturation does not restrict the set of solutions. To this end, recall the well-known link between forwarding and small-input control ([35]).

Proof. The proof is divided in three parts. It is first shown that the origin of the closed-loop system (3), (22) is globally asymptotically stable for $\delta = \delta_{\text{nom}}$. Then, it is proven that for d sufficiently large, the anti-windup effect disappears in the target equilibrium (and so regulation is achieved). Finally it is shown that the proposed design is robust to sufficiently small model parameter variations and semi-global asymptotic stability on an equilibrium is guaranteed (on which the regulation objective is satisfied).

Part 1: Global output regulation. Consider $\delta = \delta_{\text{nom}} \in \text{int}(\mathcal{S})$ and $(\mathbf{x}^*, \mathbf{u}^*) \in \mathcal{E}(\delta)$. Define the following change of coordinates:

$$\begin{pmatrix} \mathbf{u} \\ \mathbf{x} \\ \mathbf{z} \end{pmatrix} \mapsto \begin{pmatrix} u \\ x \\ z \end{pmatrix} := \begin{pmatrix} \mathbf{u} - \mathbf{u}_{\text{nom}}^* \\ \mathbf{x} - \mathbf{x}_{\text{nom}}^* \\ \mathbf{z} - \mathbf{z}_{\text{nom}}^* \end{pmatrix}$$

in which $\mathbf{z}_{\text{nom}}^* = \mathbf{0}$. In these coordinates, system (3) reads

$$\begin{aligned} \dot{x} &= \mathbf{A}(\theta)(x + \mathbf{x}_{\text{nom}}^*) + \mathbf{N}(x + \mathbf{x}_{\text{nom}}^*)(u + \mathbf{u}_{\text{nom}}^*) + \mathbf{q}(\theta), \\ &= \left(\mathbf{A}(\theta) + \sum_{j=1}^m \mathbf{N}_j \mathbf{u}_{\text{nom},j}^* \right) x + \mathbf{N}(x + \mathbf{x}_{\text{nom}}^*) u \end{aligned} \quad (23)$$

while the z -dynamics reads

$$\dot{z} = (\mathbf{C} + 2\mathbf{H}(\mathbf{x}_{\text{nom}}^*))x + \mathbf{H}(x)x,$$

for which the relations $\mathbf{C}\mathbf{x}_{\text{nom}}^* + \mathbf{H}(\mathbf{x}_{\text{nom}}^*)\mathbf{x}_{\text{nom}}^* = \mathbf{r}$ and $\mathbf{H}(x)\mathbf{x}_{\text{nom}}^* = \mathbf{H}(\mathbf{x}_{\text{nom}}^*)x$ have been used. By selecting the matrices A, B, C and the functions N, H as in the statement of the theorem, a system of the form of (9) is obtained. The following two technical lemmas show that A is Hurwitz and that the non-resonance condition $CA^{-1}B$ full rank holds. Their proofs are postponed to the Appendix.

Lemma 1. *Pick any $\delta \in \text{int}(\mathcal{S})$. Then for all $(\mathbf{x}^*, \mathbf{u}^*) \in \mathcal{E}(\delta)$, the matrix $A = \mathbf{A}(\theta) + \sum_{j=1}^m \mathbf{N}_j \mathbf{u}_j^*$ is Hurwitz.*

Lemma 2. *Pick any $\delta \in \text{int}(\mathcal{S})$. Then for all $(\mathbf{x}^*, \mathbf{u}^*) \in \mathcal{E}(\delta)$ the matrix $CA^{-1}B$ is full rank.*

Remark 2. *Lemma 1 can be understood as the natural stability of the system: in practice, for any constant duty ratio, the system stabilises to a steady-state equilibrium point. Concerning Lemma 2, it has been shown in [25] that such condition is necessary to achieve output set-point tracking in case of (sufficiently small) parametric uncertainties in every direction. Since the linearized model around the equilibrium point is stabilizable, this condition implies controllability of the extended (plant and integral action) linearised system and it is commonly referred to as “non-resonance condition” It follows from the proof of Lemma 2 that the points $\delta \in \partial\mathcal{S} := \mathcal{S} \setminus \text{int}(\mathcal{S})$ do not satisfy such a condition.*

Following the proof of Proposition 1, consider the Lyapunov function $W(x, z) = \frac{1}{2}x^\top Px + \frac{1}{2}(z - M(x))^\top \Omega(z - M(x))$ where $P = P^\top \succ 0$ verifies $PA + A^\top P \prec 0$, the function M is defined as in (14) and Ω is any symmetric positive definite matrix. Note that P always exists in view of Lemma 1. Computing the time derivative and following the same steps of the proof of Proposition 1, it follows that

$$\begin{aligned} \dot{W}(x, z) &= -\frac{1}{2}x^\top (PA + A^\top P)x - \Psi(x, z) \\ &\quad - (z - M(x))^\top \Omega \text{Dz}_d(z - M(x)) \end{aligned} \quad (24)$$

with

$$\Psi(x, z) := \psi(x, z)^\top \text{Sat}_{-\mathbf{u}_{\text{nom}}^*}^{1-\mathbf{u}_{\text{nom}}^*}(\psi(x, z))$$

with ψ defined as in the statement of the theorem, i.e. in (22). The function Ψ verifies

$$\Psi(x, z) > 0 \quad \forall (x, z) \neq (0, 0). \quad (25)$$

To show the previous inequality, let $\psi_i(x, z)$ denote the i -th element of $\psi(x, z)$. By definition of the saturation function in (1),

$$\Psi(x, z) = \sum_{i=1}^m \Psi_i(x, z) = \sum_{i=1}^m \psi_i(x, z) \text{sat}_{-\mathbf{u}_{\text{nom},i}^*}^{1-\mathbf{u}_{\text{nom},i}^*}(\psi_i(x, z))$$

and, for any $i \in \llbracket 1, m \rrbracket$, the following conditions hold:

- 1) if $\psi_i(x, z) < -\mathbf{u}_{\text{nom},i}^*$, then $\Psi_i(x, z) = -\psi_i(x, z)\mathbf{u}_{\text{nom},i}^* \geq 0$;
- 2) if $-\mathbf{u}_{\text{nom},i}^* \leq \psi_i(x, z) \leq 1 - \mathbf{u}_{\text{nom},i}^*$, then $\Psi_i(x, z) = \psi_i(x, z)^2 \geq 0$;
- 3) if $\psi_i(x, z) > 1 - \mathbf{u}_{\text{nom},i}^*$, then $\Psi_i(x, z) = \psi_i(x, z)(1 - \mathbf{u}_{\text{nom},i}^*) \geq 0$,

proving (25) since each element of the sum is positive. Moreover, since $s \text{Dz}_d(s) \geq 0$ for any s, d , it follows from (24) that $\dot{W}(x, z) \leq 0$. Since this derivative is a sum of non-negative terms, $\dot{W}(x, z) = 0$ if and only if each term is null. Moreover, $x^\top (PA + A^\top P)x = 0$ if and only if $x = \mathbf{0}$. It follows that

$$\begin{aligned} \Psi(\mathbf{0}, z) = 0 &\iff \psi_i(\mathbf{0}, z) \text{sat}_{-\mathbf{u}_{\text{nom},i}^*}^{1-\mathbf{u}_{\text{nom},i}^*}(\psi_i(\mathbf{0}, z)) \quad \forall i \in \llbracket 1, m \rrbracket \\ &\iff \psi(\mathbf{0}, z) = \mathbf{0} \iff z = M(\mathbf{0}) = \mathbf{0}, \end{aligned}$$

hence that $\dot{W}(x, z) = 0 \iff (x, z) = (\mathbf{0}, \mathbf{0})$ and that the origin of the closed-loop system is globally asymptotically stable. Following the proof of Proposition 1, it is possible to show that it is also locally exponentially stable.

Part 2: Anti-windup function design. The dead-zone function Dz_d has been introduced to implement an anti-windup in the integral action. It follows from the Lyapunov analysis that such function does not compromise the stability of the nominal closed-loop. However, the constant d must be chosen sufficiently large so that when trajectories are close to the equilibrium point for which $\mathbf{y} = \mathbf{r}$, the anti-windup has no effect (i.e. the dead-zone is equal to zero) and set-point tracking is achieved. The dead-zone constant d must therefore satisfy

$$d \geq \underline{d}, \quad \underline{d} := \sup_{(x,z) \in \mathcal{D}_z \times \mathcal{D}_M} \{ \|z - M(x)\| \}$$

where $\mathcal{D}_z, \mathcal{D}_M$ are defined as the sets containing all possible equilibrium of (x, z) . On one hand, when $\delta = \delta_{\text{nom}}$, i.e. the system converges to the nominal equilibrium, \underline{d} can be taken equal to 0 as the feed-forward action $\mathbf{u} = \mathbf{u}_{\text{nom}}^*$ is sufficient to bring the system to the equilibrium where regulation is achieved. On the other hand, when $\delta \neq \delta_{\text{nom}}$, \underline{d} must be sufficiently high: the dead-zone constant must be chosen with respect to the plant's uncertainties, so that the anti-windup effect vanishes on the (new) equilibrium point. Giving a detailed formulation of \underline{d} is cumbersome and out of the scope of the paper, as its value affects the largest admissible bounds on the set-points $\bar{\delta}$ (see Part 3 of the proof of this Theorem) and reciprocally. Its computation has therefore been omitted. For practical implementations, once a bound on the possible uncertainties for the parameters and references is known (and hence a neighbourhood of the nominal equilibrium), taking \underline{d} sufficiently high will guarantee that the anti-windup disappears on the new target equilibrium.

Such aspects have been remarked also in the experimental part in Section V. Taking \underline{d} too high will not compromise the stability or the regulation, but will simply result in a delay of the effect of the anti-windup.

Part 3: Robustness analysis. To conclude the proof of the theorem, we aim to show that for every compact set of initial conditions, there exists a bound of the parameters' uncertainty $\bar{\delta}$ such that, if $|\delta - \delta_{nom}| \leq \bar{\delta}$, then the following can still be guaranteed: i) that an equilibrium point for the closed-loop system exists; ii) that such an equilibrium is asymptotically and locally exponentially stable; iii) that the regulation task is still achieved. In this aim, let $\mathbf{w} := (\mathbf{x}, \mathbf{z})$ and let the nominal closed-loop (3), (22) be defined by

$$\dot{\mathbf{w}} = \varphi(\mathbf{w}, \delta_{nom}). \quad (26)$$

From the Lyapunov analysis in *Part 1*, there exist a radially unbounded Lyapunov function W and a positive definite function V such that

$$\frac{\partial W}{\partial w}(w) \varphi(w, \delta_{nom}) \leq -V(w) < 0$$

where $w = (\mathbf{x} - \mathbf{x}_{nom}^*, \mathbf{z} - \mathbf{z}_{nom}^*)$, for which the origin of the closed-loop is globally asymptotically stable and locally exponentially stable. Therefore, for each compact set \mathcal{D} , there exists two compact sets of initial conditions containing the origin and denoted $\underline{\mathcal{C}}$ and $\bar{\mathcal{C}}$, both in $\mathcal{X} \times \mathcal{Z}$, such that $\bar{\mathcal{C}}$ is forward invariant² for the closed-loop system (26). Therefore, by [36, Lemma 5] there exists $\rho > 0$ such that, for each C^1 vector field φ_p satisfying

$$|\varphi_p(w, \delta) - \varphi(w, \delta_{nom})| \leq \rho, \quad \forall w \in \bar{\mathcal{C}}, \quad (27)$$

$$\left| \frac{\partial \varphi_p}{\partial x}(w, \delta) - \frac{\partial \varphi}{\partial x}(w, \delta_{nom}) \right| \leq \rho, \quad \forall w \in \underline{\mathcal{C}}, \quad (28)$$

there exists an exponentially stable equilibrium of

$$\dot{w} = \varphi_p(w, \delta),$$

whose basin of attraction contains the compact set $\bar{\mathcal{C}}$. Let us define now the function $\bar{\rho} : \mathcal{D} \rightarrow \mathbb{R}_{>0}$ as

$$\bar{\rho}(\delta) := \max_{w \in \bar{\mathcal{C}}} \left\{ |\varphi(w, \delta) - \varphi(w, \delta_{nom})|, \left| \frac{\partial \varphi}{\partial x}(w, \delta) - \frac{\partial \varphi}{\partial x}(w, \delta_{nom}) \right| \right\}.$$

Such a function is continuous and satisfies $\bar{\rho}(\delta_{nom}) = 0$. Any positive real number $\bar{\delta} > 0$ can now be selected such that, $|\delta - \delta_{nom}| \leq \bar{\delta}$ implies $\bar{\rho}(\delta) \leq \rho$. This parameter $\bar{\delta} > 0$ is a solution to the third part of the proof. Indeed, for each δ such that $|\delta - \delta_{nom}| \leq \bar{\delta}$, then the closed loop system

$$\dot{w} = \varphi(w, \delta),$$

satisfies (27) and (28) and consequently admits an exponentially stable equilibrium with a basin of attraction containing $\mathcal{D} \times \{0\}$. Thanks to the integral action, the output set-point tracking is achieved on this equilibrium, which concludes the proof. \square

Remark 3. A more precise characterisation of the robustness bound $\bar{\delta}$ can be given by explicitly computing its value. Indeed

²Simply pick $\bar{\mathcal{C}} = \{(x, z) : W(x, z) \leq c_0\}$ for sufficiently large c_0 .

the closed-loop is a polynomial system, hence computation solvers or polynomial optimisation tools (see [37], [38]) could be used.

C. Tuning of the control gains

The proposed control law $\alpha(\mathbf{x}, \mathbf{z})$ in (22) admits some free-to-choose parameters. In particular, any matrices $P = P^\top$ satisfying (10) and $\Omega = \Omega^\top \succ 0$ could be selected. The aim of this section is to give guidelines for choosing the matrices P and Ω with regard to some cost function around the nominal equilibrium point. Consider the nominal system (3), (22) with $\delta = \delta_{nom}$. Since only local performance is sought around the nominal equilibrium, the tuning procedure is designed without taking into account the saturation function and the dead-zone anti-windup, as these functions have no effect sufficiently close to the equilibrium point. Taking the nominal error coordinates $(\mathbf{x}, \mathbf{z}) \mapsto (x, z) = (\mathbf{x} - \mathbf{x}_{nom}^*, \mathbf{z} - \mathbf{z}_{nom}^*)$, the closed-loop system writes

$$\begin{aligned} \dot{x} &= Ax + (N(x) + B)u \\ \dot{z} &= Cx + H(x)x \\ u &= \psi(x, z) \end{aligned} \quad (29)$$

where $u = \mathbf{u} - \mathbf{u}_{nom}^*$, A, B, N, C and H are taken as in Theorem 1 and $\psi(\cdot)$ is taken accordingly to Proposition 1.

Consider the cost function $\mathcal{J} : \mathbb{R}^n \times \mathbb{R}^m \rightarrow \mathbb{R}_{>0}$ defined as

$$\mathcal{J} := \int_0^\infty \left[w^\top(t) \tilde{Q} w(t) + u^\top(t) \tilde{R} u(t) \right] dt \quad (30)$$

for some given matrices $\tilde{Q} = \tilde{Q}^\top \succeq 0$ and $\tilde{R} = \tilde{R}^\top \succ 0$, where $w(t) = (x(t), z(t))$ is the trajectory of the closed-loop at time t for some initial conditions. Consider the linearisation of the closed-loop system (29) around $w = (x, z) = (0, 0)$:

$$\begin{aligned} \dot{\tilde{w}} &= \tilde{A} \tilde{w} + \tilde{B} \tilde{u} \\ \tilde{u} &:= \tilde{K} \tilde{w} \end{aligned} \quad (31)$$

where $\tilde{w} \in \mathbb{R}^{n+m}$, $\tilde{u} \in \mathbb{R}^m$ and

$$\begin{aligned} \tilde{A} &:= \begin{bmatrix} A & 0 \\ C & 0 \end{bmatrix}, \quad \tilde{B} := \begin{bmatrix} B \\ 0 \end{bmatrix} \\ \tilde{K} &:= -[B^\top P + B^\top M_0^\top \Omega M_0 \quad -B^\top M_0^\top \Omega] \end{aligned} \quad (32)$$

For a linear system of the form (31), a linear state-feedback optimal control law ([39, Section 3.12]) is given by

$$\tilde{u} = \tilde{K}_{opt} \tilde{w} = -\tilde{R}^{-1} \tilde{B}^\top \tilde{S} \tilde{w} \quad (33)$$

where $\tilde{S} = \tilde{S}^\top \succ 0$ is the solution of the algebraic Riccati equation

$$\tilde{S} \tilde{A} + \tilde{A}^\top \tilde{S} - \tilde{S} \tilde{B} \tilde{R}^{-1} \tilde{B}^\top \tilde{S} = -\tilde{Q} \quad (34)$$

The idea is to choose the control law degrees of freedom such that its linearisation \tilde{K} is as close as possible to the optimal control law for linear systems \tilde{K}_{opt} . In this sense, it can be rewritten as an optimisation problem of the form

$$\begin{aligned} \min_{P, \Omega, \varepsilon} \quad & \varepsilon \\ \text{s.t.} \quad & (\tilde{K} - \tilde{K}_{opt})(\tilde{K} - \tilde{K}_{opt})^\top - \varepsilon \mathbf{Id}_m \preceq \mathbf{0} \\ & P \succ \mathbf{0}, \quad \Omega \succ \mathbf{0}, \quad \varepsilon \geq 0 \\ & A^\top P + PA \prec \mathbf{0} \end{aligned} \quad (35)$$

where \tilde{K} depends on P and Ω , as seen in (32). This problem can be expressed in LMI form using the Schur complement:

$$\begin{aligned} & \min_{P, \Omega, \varepsilon} \varepsilon \\ \text{s.t.} & \begin{bmatrix} -\varepsilon \mathbf{Id}_m & (\tilde{K} - \tilde{K}_{opt}) \\ (\tilde{K} - \tilde{K}_{opt})^\top & -\mathbf{Id} \end{bmatrix} \preceq \mathbf{0} \\ & P \succ \mathbf{0}, \Omega \succ \mathbf{0}, \varepsilon \geq 0 \\ & A^\top P + PA \prec \mathbf{0} \end{aligned}$$

which is a semi-definite program for which efficient solvers exist, see for instance [37], [38], [40].

Remark 4. *As the system's dynamics involve the plant and the integrator, in most applications there is no interest in choosing the cost function to be dependent on the full state space, i.e. \tilde{Q} is generally positive semi-definite. Hence one can select $\tilde{Q} := \tilde{C}^\top \tilde{C}$ for some matrix \tilde{C} of appropriate dimensions, where (\tilde{A}, \tilde{C}) is assumed to be detectable to still provide convergence of the closed-loop system towards an equilibrium point. Moreover, note that the plant's uncertainties play a role in this tuning, suggesting that more advanced techniques could be used, such as robust optimal control or stochastic optimal control. As this focus is out of the main scope of this work, the details will not be explained, and the interested readers may refer for instance to [41]–[43] and the references therein.*

V. EXPERIMENTATIONS

This section presents tenth scale experimental measurements of the PFC in closed-loop with the proposed controller. The experimental setup is presented in Fig. 4 and 5. A dSPACE MicroLabBox rapid prototyping system (μLB) is used to control the PFC. A voltage-controlled electronic load in series with a resistor (EL+R) is connected to the first terminal of the PFC through thirty metres of standard U1000 RV2 cable (L_G). The two other terminals are connected to a resistor (R) and a power supply (PS), also through thirty metres of the same cable.

The proposed controller is tested through different scenarios. First, it is verified that the control objectives can be properly reached, despite perturbations of the uncertain parameters. Second, a test is performed to show the efficiency of the anti-windup function. Third, an experiment illustrates the effect of the proposed tuning of the parameters. Finally, the generalisation to m -terminal is illustrated by a simulation on MATLAB Simulink, for $m = 5$.

Unless otherwise stated, the parameters of control law (22) are selected as follows: the matrices P and M_i , $i \in \llbracket 1, p \rrbracket$ are computed using CVX, a package for specifying and solving convex programs [44],[45], such that

$$\begin{aligned} A(\theta_{nom})^\top P + PA(\theta_{nom}) &\preceq -\mathbf{Id}_n, \\ M_i A(\theta_{nom}) + A^\top(\theta_{nom}) M_i &= \frac{1}{2}(H_i + H_i^\top), \end{aligned}$$

the function ψ in (22) is multiplied by a scalar positive gain $\kappa = 0.01$ inside the saturation (see Remark 1) and the tuning matrix Ω is chosen equal to $\text{diag}\{[1, 1, 5]\}$. These values have been found by experimentally tuning the parameters to reach satisfactory dynamics.

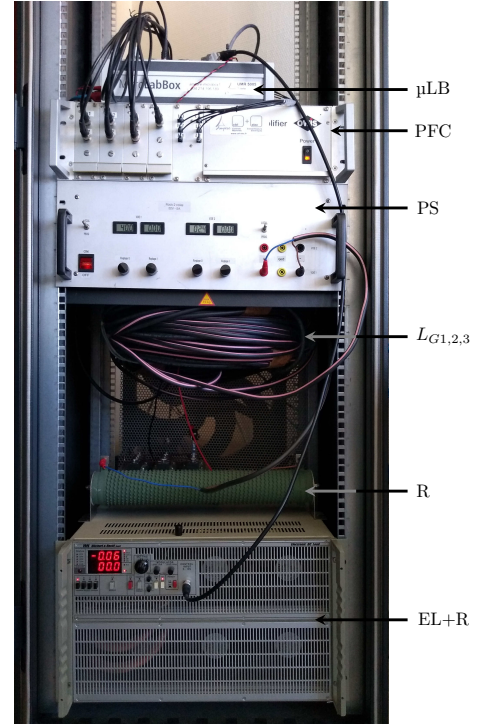


Fig. 4. Picture of the experimental setup

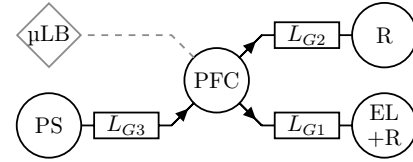


Fig. 5. Drawing of the experimental setup

A. Robust Regulation

The system is initialised on the nominal set-point $\delta_{nom} = (\theta_{nom}, r_{nom})$, whose numerical values are displayed in Table III. At $t = 21$ ms, the reference is changed to r_a , and at $t = 61.5$ ms, the system is perturbed with a voltage step on the electronic load, from 2 V to 10 V, so that $\theta = \theta_a$ (see Table III). From Fig. 6, it can be concluded that the objectives are properly reached in 20 ms, so that modelling and measurement errors are properly compensated for. Moreover, observe that although no reference is tracked on the third line, a constant power value is asymptotically reached. This asymptotic value is determined by the total power balance, so that it equals $-\mathbf{P}_1^r - \mathbf{P}_2^r$ plus the power losses in the converter.

B. Saturation and anti-windup

Since the control law does not exhibit large oscillations with the proposed tuning, it not possible to illustrate the effect of transient saturations and of the anti-windup term. Moreover, it is assumed in the theoretical developments that all given references are reachable (i.e. belong to \mathcal{S}). However, bearing in mind that in practice the power references are given by a higher-layer control algorithm, observe that if a constant perturbation occurring on a line makes the given reference

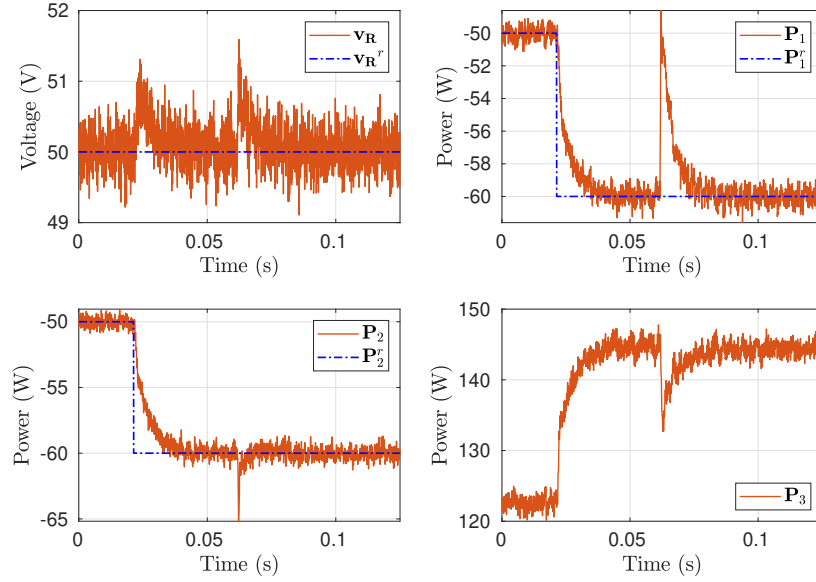


Fig. 6. Experimental measurements of the PFC in closed-loop with control (22). Reservoir voltage and power in each line with their references

TABLE III
Set-point numerical values

Parameter		Test value			Unit
		$k = 1$	$k = 2$	$k = 3$	
θ_{nom}	L_{Gk}	18	18	18	μH
	R_{Gk}	21.7	24.5	1.2	Ω
	V_{Gk}	2	0	40	V
θ_a	L_{Gk}	18	18	18	μH
	R_{Gk}	21.7	24.5	1.2	Ω
	V_{Gk}	10	0	40	V

Parameter		Test value		Unit
\mathbf{r}_{nom}	\mathbf{P}_1^r	-50	W	
	\mathbf{P}_2^r	-50	W	
	$\mathbf{v}_{\mathbf{R}}^r$	50	V	
\mathbf{r}_a	\mathbf{P}_1^r	-60	W	
	\mathbf{P}_2^r	-60	W	
	$\mathbf{v}_{\mathbf{R}}^r$	50	V	

unreachable, it will induce a saturation of the duty cycle and lead to an integral wind-up, until the higher-layer controller is able to deliver a new attainable reference. This scenario has been tested and the most relevant signals are displayed in Fig. 7. \mathbf{P}_1^r is set to -85 W, which is attainable when $V_{G1} = 2$ V, but not when $V_{G1} = 10$ V. Such a step on V_{G1} is implemented via the electronic load at $t = 0.1$ s. This prevents the power reference to be reached due to duty cycle constraints. Assume that the higher-layer controller delivers a new *reachable* reference $\mathbf{P}_1^r = -75$ W at $t = 0.5$ s. Without anti-windup action, i.e. $\zeta = 0$ on (8), the value of \mathbf{z}_1 increases continuously, and the integral wind-up problem is clearly illustrated as the tracking capability is only recovered after 600 ms (in blue). This is in contrast with $\mathbf{z}_{1,AW}$ which saturates around 0.2 J, leading to a much faster recovery of the tracking capability (in red).

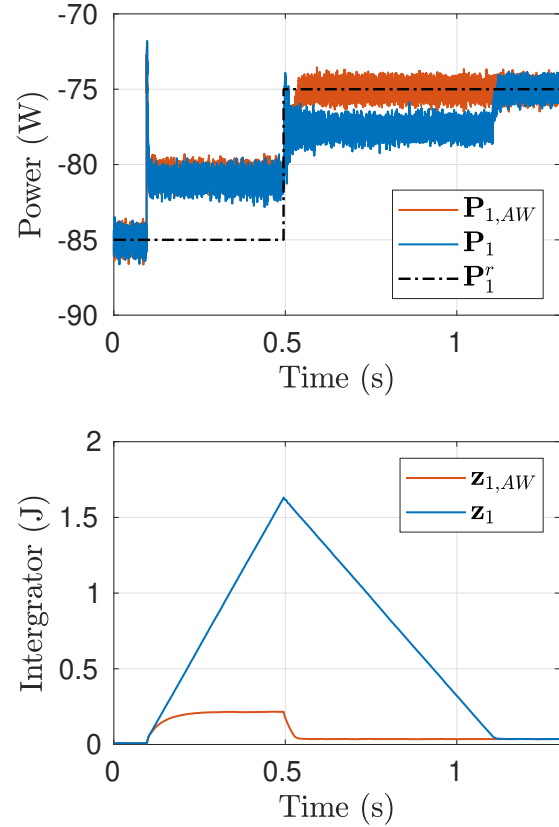


Fig. 7. Experimental measurements illustrating the efficiency of the dead-zone function method to prevent an integral wind-up when the set-point is unreachable. Power on the first line with its reference (top) and corresponding integrator (bottom)

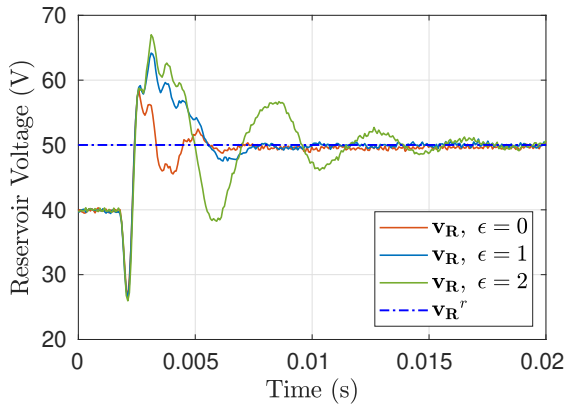


Fig. 8. Experimental measurements of the startup of the converter on the nominal set-point for different values of $\Omega = \epsilon \mathbf{Id}_3$. Only \mathbf{v}_R is shown, but the same behaviour is observed on the other outputs

C. Evaluation of the tuning method

In Section IV-C, a procedure is given to assist the tuning of the control parameters: define a cost function in (30), solve the Riccati equation in (34) and deduce the control gain using (33). Then, chose P and Ω along the optimisation problem (35). This procedure has been followed: for simplicity, the cost function is chosen using the matrices $\tilde{Q} = \mathbf{Id}_{13}$ and $\tilde{R} = 0.01 \times \mathbf{Id}_3$. Indeed, since the inputs are saturated duty cycles, there is no need to minimise their magnitude, so the associated cost is small. The Riccati equation has been solved using the `icare`(\cdot) function in MATLAB.

In order to evaluate the impact of Ω , matrix P is kept unchanged while different values for Ω are tested with the optimisation problem. One then notices that for $\Omega = \epsilon \mathbf{Id}_3$, smaller values of ϵ lead to a smaller ε , i.e. \tilde{K} is closer to \tilde{K}_{opt} . This is verified during a startup test on the nominal system. Considering $(\theta_{nom}, \mathbf{r}_{nom})$ given by Table III at $t = 2$ ms, the reservoir voltage transients are displayed in Fig. 8 for different ϵ . It can clearly be noticed that decreasing the value of Ω improves the dynamics on the nominal set-point. However, note that this matrix multiplies the integral part \mathbf{z} of the current law (see (12)). Therefore, the selection of Ω appears to be a trade-off between nominal performance, suggesting $\Omega = \mathbf{0}$, and accuracy of the steady-state, requiring $\Omega \succ \mathbf{0}$.

D. Simulation of a 5-terminal PFC

This paper generalises the control law from [9] to m branches. A MATLAB-Simulink simulation validates this extension for $m = 5$. The two new branches have the same parameters and references as branches one and two and have been inserted between the second and the third ones, i.e. they are numbered 3 and 4. Thus, the numerical values are $L_{G1,2,3,4,5} = 18 \mu\text{H}$, $R_{G1,3} = 21.7 \Omega$, $R_{G2,4} = 24.5 \Omega$, $R_{G5} = 1.2 \Omega$, $V_{G2,4} = 0 \text{ V}$ and $V_{G5} = 40 \text{ V}$. $V_{G1,3}$ is initially set to 2 V and changed to 10 V at $t = 61.5$ ms. The power references are all initially at $\mathbf{P}_{1,2,3,4}^r = -50 \text{ W}$, and stepped to -60 W at $t = 21$ ms. The reservoir voltage reference \mathbf{v}_R^r remains at 50 V.

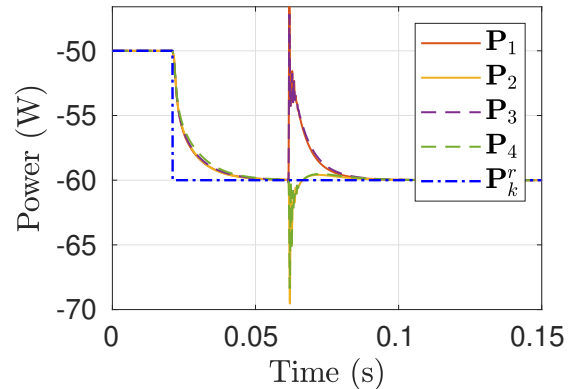
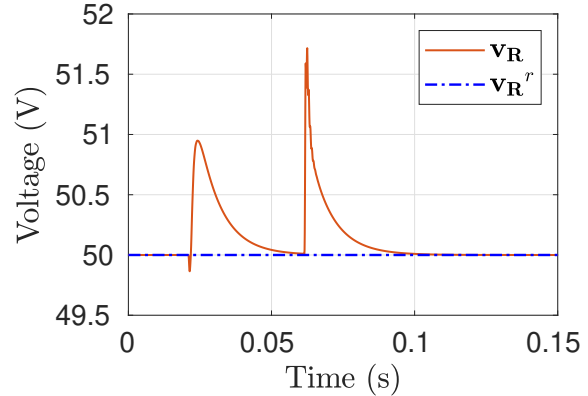


Fig. 9. Simulation of the PFC model (3) for $m = 5$, in closed-loop with control (22). Reservoir voltage and power in the $m - 1$ first lines with their references

The resulting reservoir voltage and power signals are drawn in Fig. 9. Their comparison to those of Fig. 6, shows that the proposed model is able to accurately capture the dynamics of the system. Furthermore, this simulation suggests that the generalisation of the control law to more than three terminals maintains both the stability and the performance of the system.

VI. CONCLUSION

A robust controller has been designed for an m -terminal PFC ensuring the regulation of the electrical power in each line of the node, while explicitly taking into account the saturation constraints of the duty cycles. The control law is made of an integral action processing the regulation error, and a stabiliser for the resulting cascade system is designed via forwarding techniques. An input saturation function is included to meet the physics of the system and an anti-windup design is added to prevent a possible instability caused by this saturation. A procedure to tune the controller with respect to a cost function is then presented. An experimental setup for a 3-branch PFC has been built to show the validity of the proposed control law. The experiments show the robustness of the proposed design, as well as the performance of the anti-windup action and the tuning method. Moreover, simulations on a 5-branch PFC have been implemented to shown the validity of the extension of the control law to any m -terminal PFC.

The application of the control problem requires a stability of the closed-loop system for a very large domain in the parametric and references spaces. Future studies will involve finding other methods to enhance the robustness of the proposed design, involving the choice of an optimal nominal set-point and numerical simulations.

APPENDIX

A. Proof of Proposition 2

By considering (3) and posing $\dot{\mathbf{x}} = 0$, the following set of equations is found

$$\begin{cases} \sum_{k=1}^m \mathbf{i}_k^* \mathbf{u}_k^* = 0, & (36a) \\ \mathbf{v}_k^* - \mathbf{v}_R^* \mathbf{u}_k^* = 0, & (36b) \\ -\mathbf{i}_k^* + \mathbf{i}_{Gk}^* = 0, & (36c) \\ -\mathbf{v}_k^* - R_{Gk} \mathbf{i}_{Gk}^* + V_{Gk} = 0, & (36d) \end{cases}$$

where $k \in \llbracket 1, m \rrbracket$, and

$$\begin{cases} \mathbf{v}_k^* \mathbf{i}_{Gk}^* = \mathbf{P}_k^r, & k \in \llbracket 1, m-1 \rrbracket \\ \mathbf{v}_R^* = \mathbf{v}_R^r. \end{cases} \quad (37a)$$

$$\begin{cases} \mathbf{v}_R^* = \mathbf{v}_R^r. \end{cases} \quad (37b)$$

Solving (36b) and (36c) results in

$$\mathbf{u}_k^* = \frac{\mathbf{v}_k^*}{\mathbf{v}_R^*} \quad \text{and} \quad \mathbf{i}_k^* = \mathbf{i}_{Gk}^* \quad (38)$$

where $\mathbf{v}_R^* = \mathbf{v}_R^r > 0$. Hence the first condition for the existence of solutions is $0 \leq \frac{\mathbf{v}_k^*}{\mathbf{v}_R^*} \leq 1$. Feeding (36c) into (36a) leads to

$$\frac{1}{\mathbf{v}_R^*} \sum_{k=1}^m \mathbf{i}_{Gk}^* \mathbf{v}_k^* = 0. \quad (39)$$

Taking (37) in (39) results in

$$\frac{1}{\mathbf{v}_R^r} \left(\sum_{k=1}^{m-1} \mathbf{P}_k^r + \mathbf{i}_{Gm}^* \mathbf{v}_m^* \right) = 0, \quad (40)$$

from which $\mathbf{P}_m^r := -\sum_{k=1}^{m-1} \mathbf{P}_k^r = \mathbf{i}_{Gm}^* \mathbf{v}_m^*$ is defined. Then, multiplying (36d) by \mathbf{v}_k^* and using (37a), it follows that

$$-(\mathbf{v}_k^*)^2 + V_{Gk} \mathbf{v}_k^* - R_{Gk} \mathbf{P}_k^r = 0 \quad (41)$$

hence the second condition for the existence of real solutions is $\Delta_k(\delta) = V_{Gk}^2 - 4R_{Gk} \mathbf{P}_k^r \geq 0$. If $\Delta_k(\delta) \geq 0$, the characterisation of $\mathcal{E}(\delta)$ can be given using (36) and (37) as

$$\mathcal{E}(\delta) = \begin{cases} \mathbf{v}_k^* = \frac{1}{2} \left(V_{Gk} \pm \sqrt{\Delta_k(\delta)} \right) & (42a) \\ \mathbf{i}_k^* = \mathbf{i}_{Gk}^* = \frac{1}{R_{Gk}} (V_{Gk} - \mathbf{v}_k^*) & (42b) \\ \mathbf{v}_R^* = \mathbf{v}_R^r & (42c) \\ \mathbf{u}_k^* = \frac{\mathbf{v}_k^*}{\mathbf{v}_R^r} & (42d) \end{cases}$$

with $k \in \llbracket 1, m \rrbracket$ and $\mathbf{v}_R^r > 0$ by definition of \mathcal{R} . \square

B. Proof of Lemma 1

To show that A is Hurwitz, it is sufficient to show that the origin of the system $\dot{x} = Ax$ is globally asymptotically stable. Taking the quadratic Lyapunov function $V_J(x) = x^T \mathbf{J}(\theta) x$ yields

$$\begin{aligned} \dot{V}_J(x) &= x^T (A^T \mathbf{J}(\theta) + \mathbf{J}(\theta) A) x \\ &= -x^T \text{diag} \{ \mathbf{0}_{n-m}^T, R_{G1}, \dots, R_{Gm} \} x \leq 0 \end{aligned}$$

by definition of Θ . By applying LaSalle's invariance principle, the system converges to the following set $\{x : \dot{V}_J(x) = 0\} = \text{Im}\{[\mathbf{I}_{n-m} \ \mathbf{0}_{(n-m) \times m}]^T\}$. Pick any element x so that $i_{Gk} \equiv 0$, for all $k \in \llbracket 1, m \rrbracket$. Plugging it in the i_{Gk} -dynamic, see (4a) results in

$$0 \equiv \frac{d}{dt} i_{Gk} = -\frac{1}{L_{Gk}} v_k,$$

which leads to $v_k \equiv 0$. From the v_k -dynamic this means

$$0 \equiv \frac{d}{dt} v_k = -\frac{1}{C} i_k,$$

and so $i_k \equiv 0$. Finally, by looking at the i_k -dynamic, the following holds

$$0 \equiv \frac{d}{dt} i_k = -\frac{1}{L} \mathbf{u}_k^* v_R.$$

Before concluding that $v_R \equiv 0$, it is necessary to prove that $(\mathbf{u}_1^*, \dots, \mathbf{u}_m^*) \neq (0, \dots, 0)$. From (42d) and the definition of \mathcal{R} , a necessary and sufficient condition is $(\mathbf{v}_1^*, \dots, \mathbf{v}_m^*) \neq (0, \dots, 0)$. From (42a), and the definition of Θ , \mathbf{v}_k^* equals zero on two conditions: The first one is $V_{Gk} = 0$ and $\Delta_k = 0$, which is excluded by taking $(\delta) \in \text{int}(\mathcal{S})$. The second one is $V_{Gk} - \sqrt{V_{Gk}^2 - 4R_{Gk} \mathbf{P}_k^r} = 0$, which occurs if and only if $\mathbf{P}_k^r = 0$, by definition of Θ . Yet, the definition of \mathcal{R} ensures that $(\mathbf{P}_1^r, \dots, \mathbf{P}_{m-1}^r) \neq (0, \dots, 0)$, meaning there is at least one $\mathbf{u}_k^* \neq 0$ and so $v_R \equiv 0$ for all $(\theta, r) \in \text{int}(\mathcal{S})$, which concludes the proof. \square

C. Proof of Lemma 2

As the number of inputs equals the number of outputs, $CA^{-1}B$ is full rank if and only if the following matrix is injective:

$$T = \begin{bmatrix} A & B \\ C & \mathbf{0} \end{bmatrix}$$

Let us show that $T[x^T, u^T]^T = \mathbf{0} \iff [x^T, u^T]^T = \mathbf{0}$

$$Ax + Bu = \mathbf{0} \iff \begin{cases} \frac{1}{C_R} \sum_{j=1}^m \mathbf{u}_j^* i_j + \mathbf{i}_k^* u_k = 0 & (43a) \\ \frac{1}{L} (-\mathbf{u}_k^* v_R + v_k - \mathbf{v}_R^r u_k) = 0 & (43b) \\ \frac{1}{C} (-i_k + i_{Gk}) = 0 & (43c) \\ \frac{1}{L_{Gk}} (-v_k - R_{Gk} i_{Gk}) = 0 & (43d) \end{cases}$$

$$Cx = \mathbf{0} \iff \begin{cases} 2\left(\frac{i_{Gk}^*}{2} v_k + \frac{\mathbf{v}_k^*}{2} i_{Gk}\right) = 0, \quad k \in \llbracket 1, m-1 \rrbracket & (43e) \\ v_R = 0 & (43f) \end{cases}$$

Using (43b), (43c), (43d) and (43f), one gets

$$v_k = \mathbf{v}_R^r u_k, \quad i_k = i_{Gk} \quad \text{and} \quad v_k = -R_{Gk} i_{Gk}. \quad (44)$$

Placing the latter in (43e) yields

$$(-R_{Gk} \mathbf{i}_{Gk}^* + \mathbf{v}_k^*) i_{Gk} = 0, \quad k \in \llbracket 1, m-1 \rrbracket.$$

Using (36d): $-R_{Gk} \mathbf{i}_{Gk}^* = -V_{Gk} + \mathbf{v}_k^*$ then gives

$$(-V_{Gk} + 2\mathbf{v}_k^*) i_{Gk} = 0, \quad k \in \llbracket 1, m-1 \rrbracket$$

and, from (42a): $\mathbf{v}_k^* = \frac{1}{2} \left(V_{Gk} \pm \sqrt{\Delta_k(\delta)} \right)$, one finds

$$\pm i_{Gk} \sqrt{\Delta_k(\theta, \mathbf{r})} = 0, \quad k \in \llbracket 1, m-1 \rrbracket.$$

In $\text{int}(\mathcal{S})$, $\Delta_j(\theta, \mathbf{r}) > 0$, hence $i_{Gk} = 0$. Remembering that by definition of Θ and \mathcal{R} , $R_{Gk} > 0$ for $k \in \llbracket 1, m \rrbracket$ and $\mathbf{v}_{\mathbf{R}}^r > 0$ and using (44), it can be concluded that $v_k = i_k = u_k = 0$, $k \in \llbracket 1, m-1 \rrbracket$. Using (43a), yields

$$\frac{1}{C_{\mathbf{R}}} (\mathbf{u}_m^* i_m + \mathbf{i}_m^* u_m) = 0, \quad (45)$$

$$\stackrel{(44)}{\iff} \mathbf{u}_m^* i_m - \mathbf{i}_m^* \frac{R_{Gm}}{\mathbf{v}_{\mathbf{R}}^r} i_m = 0, \quad (46)$$

$$\stackrel{(42d),(42b)}{\iff} \frac{\mathbf{v}_m^*}{\mathbf{v}_{\mathbf{R}}^r} i_m - \frac{1}{\mathbf{v}_{\mathbf{R}}^r} (V_{Gm} - \mathbf{v}_m^*) i_m = 0, \quad (47)$$

$$\stackrel{(42a)}{\iff} \frac{1}{\mathbf{v}_{\mathbf{R}}^r} \left(\sqrt{\Delta_k(\delta)} \right) = 0. \quad (48)$$

Again, since $\mathbf{v}_{\mathbf{R}}^r > 0$ and $\Delta_k(\delta) > 0 \forall \delta \in \text{int}(\mathcal{S})$, it follows that $i_m = 0$, hence that $i_{Gm} = v_m = u_m = 0$ by (44), and $[x^T, u^T]^T = \mathbf{0}$. It can therefore be concluded that T is full rank for all $(\theta, \mathbf{r}) \in \text{int}(\mathcal{S})$. \square

REFERENCES

- [1] S. Sen and V. Kumar, "Microgrid control: A comprehensive survey," *Annual Reviews in control*, vol. 45, pp. 118–151, 2018.
- [2] T. Simon, J.-F. Tréguët, X. Lin-Shi, and H. Morel, "Modelling and Control of a Power Flow Controller for DC Microgrids," in *2021 23rd European Conference on Power Electronics and Applications (EPE'21 ECCE Europe)*. IEEE, 2021.
- [3] L. Mackay, T. Hailu, L. Ramirez-Elizondo, and P. Bauer, "Decentralized current limiting in meshed dc distribution grids," in *2015 IEEE First International Conference on DC Microgrids (ICDCM)*. IEEE, 2015, pp. 234–238.
- [4] I. Zafeiratou, I. Prodan, L. Lefèvre, and L. Piétrac, "Dynamical modelling of a dc microgrid using a port-hamiltonian formalism," *IFAC-PapersOnLine*, vol. 51, no. 2, pp. 469–474, 2018.
- [5] S. Balasubramaniam, C. E. Ugalde-Loo, and J. Liang, "Series current flow controllers for dc grids," *IEEE Access*, vol. 7, pp. 14 779–14 790, 2019.
- [6] Y. Takahashi, K. Natori, and Y. Sato, "A multi-terminal power flow control method for next-generation dc power network," in *2015 IEEE Energy Conversion Congress and Exposition (ECCE)*. IEEE, 2015, pp. 6223–6230.
- [7] K. Natori, Y. Nakao, and Y. Sato, "A novel control approach to multi-terminal power flow controller for next-generation dc power network," in *2018 International Power Electronics Conference (IPEC-Niigata 2018-ECCE Asia)*. IEEE, 2018, pp. 588–592.
- [8] M. Barara, H. Morel, and C. Guy, "Control strategy scheme for consistent power flow control in meshed dc micro-grids," in *COSYS-DC, International Conference on Components and Systems do DC Grids. Grenoble, France, 2017*.
- [9] T. Simon, M. Giaccagli, J.-F. Tréguët, D. Astolfi, V. Andrieu, X. Lin-Shi, and H. Morel, "Robust Output Set-Point Tracking for a Power Flow Controller via Forwarding Design," in *2021 60th IEEE Conference on Decision and Control (CDC)*, 2021.
- [10] D. Koditschek and K. Narendra, "Stabilizability of second-order bilinear systems," *IEEE Transactions on Automatic Control*, vol. 28, no. 10, pp. 987–989, 1983.
- [11] P.-O. Gutman, "Stabilizing controllers for bilinear systems," *IEEE Transactions on Automatic Control*, vol. 26, no. 4, pp. 917–922, 1981.
- [12] J. P. Quinn, "Stabilization of bilinear systems by quadratic feedback controls," *Journal of Mathematical Analysis and Applications*, vol. 75, no. 1, pp. 66–80, 1980.
- [13] R. Longchamp, "Stable feedback control of bilinear systems," *IEEE Transactions on Automatic Control*, vol. 25, no. 2, pp. 302–306, 1980.
- [14] S. P. Banks, "Stabilizability of finite-and infinite-dimensional bilinear systems," *IMA Journal of Mathematical Control and Information*, vol. 3, no. 4, pp. 255–271, 1986.
- [15] S. Tarbouriech, I. Queinnec, T. Calliero, and P. Peres, "Control design for bilinear systems with a guaranteed region of stability: An lmi-based approach," in *2009 17th Mediterranean Conference on Control and Automation*. IEEE, 2009, pp. 809–814.
- [16] V. Andrieu and S. Tarbouriech, "Global asymptotic stabilization for a class of bilinear systems by hybrid output feedback," *IEEE Transactions on Automatic Control*, vol. 58, no. 6, pp. 1602–1608, 2012.
- [17] O. M. Grasselli, A. Isidori, and F. Nicolo, "Output regulation of a class of bilinear systems under constant disturbances," *Automatica*, vol. 15, no. 2, pp. 189–195, 1979.
- [18] R. Cisneros, M. Pirro, G. Bergna, R. Ortega, G. Ippoliti, and M. Molinas, "Global tracking passivity-based pi control of bilinear systems: Application to the interleaved boost and modular multilevel converters," *Control Engineering Practice*, vol. 43, pp. 109–119, 2015.
- [19] G. Tang, Y. Zhao, and H. Ma, "Optimal output tracking control for bilinear systems," *Transactions of the Institute of Measurement and Control*, vol. 28, no. 4, pp. 387–397, 2006.
- [20] B. Zitte, B. Hamroun, D. Astolfi, and F. Couenne, "Robust control of a class of bilinear systems by forwarding: Application to counter current heat exchanger," in *21st IFAC World Congress*, 2020.
- [21] L. Guo and H. Schwarz, "A control scheme for bilinear systems and application to a secondary controlled hydraulic rotary drive," in *Proceedings of the 28th IEEE Conference on Decision and Control*, IEEE, 1989, pp. 542–547.
- [22] D. Williamson, "Observation of bilinear systems with application to biological control," *Automatica*, vol. 13, no. 3, pp. 243–254, 1977.
- [23] P. M. Pardalos and V. A. Yatsenko, *Optimization and Control of Bilinear Systems: Theory, Algorithms, and Applications*. Springer Science & Business Media, 2010, vol. 11.
- [24] F. Mazenc and L. Praly, "Adding integrations, saturated controls, and stabilization for feedforward systems," *IEEE Transactions on Automatic Control*, vol. 41, no. 11, pp. 1559–1578, 1996.
- [25] D. Astolfi and L. Praly, "Integral Action in Output Feedback for Multi-Input Multi-Output Nonlinear Systems," *IEEE Transactions on Automatic Control*, vol. 62, no. 4, pp. 1559–1574, Apr. 2017.
- [26] F. Poulain and L. Praly, "Robust asymptotic stabilization of nonlinear systems by state feedback," *IFAC Proceedings Volumes*, vol. 43, no. 14, pp. 653–658, Sep. 2010.
- [27] M. Giaccagli, D. Astolfi, V. Andrieu, and L. Marconi, "Sufficient conditions for output reference tracking for nonlinear systems: a contractive approach," in *2020 59th IEEE Conference on Decision and Control (CDC)*. IEEE, 2020, pp. 4580–4585.
- [28] —, "Sufficient conditions for global integral action via incremental forwarding for input-affine nonlinear systems," *IEEE Transactions on Automatic Control*, 2021.
- [29] —, "Incremental stabilization of cascade nonlinear systems and harmonic regulation: a forwarding-based design," *Prov. accepted in IEEE Transactions on Automatic Control*, 2022.
- [30] L. Praly, R. Ortega, and G. Kaliora, "Stabilization of nonlinear systems via forwarding mod $\{L_g V\}$," *IEEE Transactions on Automatic Control*, vol. 46, no. 9, pp. 1461–1466, 2001.
- [31] B. A. Francis and W. M. Wonham, "The internal model principle of control theory," *Automatica*, vol. 12, no. 5, pp. 457–465, 1976.
- [32] S. Tarbouriech and M. Turner, "Anti-windup design: an overview of some recent advances and open problems," *IET control theory & applications*, vol. 3, no. 1, pp. 1–19, 2009.
- [33] A. Zheng, M. V. Kothare, and M. Morari, "Anti-windup design for internal model control," *International Journal of Control*, vol. 60, no. 5, pp. 1015–1024, 1994.
- [34] S. Galeani, S. Tarbouriech, M. Turner, and L. Zaccarian, "A tutorial on modern anti-windup design," *European Journal of Control*, vol. 15, no. 3–4, pp. 418–440, 2009.
- [35] G. Kaliora and A. Astolfi, "On the stabilization of feedforward systems with bounded control," *Systems & Control Letters*, vol. 54, no. 3, pp. 263–270, Mar. 2005. [Online]. Available: <https://linkinghub.elsevier.com/retrieve/pii/S0167691104001380>
- [36] D. Astolfi and L. Praly, "Integral action in output feedback for multi-input multi-output nonlinear systems," *IEEE Transactions on Automatic Control*, vol. 62, no. 4, pp. 1559–1574, 2016.
- [37] D. Henrion and J.-B. Lasserre, "Gloptipoly: Global optimization over polynomials with matlab and sedumi," *ACM Transactions on Mathematical Software (TOMS)*, vol. 29, no. 2, pp. 165–194, 2003.
- [38] D. Henrion, J.-B. Lasserre, and J. Löfberg, "Gloptipoly 3: moments, optimization and semidefinite programming," *Optimization Methods & Software*, vol. 24, no. 4–5, pp. 761–779, 2009.
- [39] D. E. Kirk, *Optimal control theory: an introduction*. Courier Corporation, 2004.

- [40] J. G. VanAntwerp and R. D. Braatz, "A tutorial on linear and bilinear matrix inequalities," *Journal of process control*, vol. 10, no. 4, pp. 363–385, 2000.
- [41] R. Van Handel, "Stochastic calculus, filtering, and stochastic control," *Course notes*, URL <http://www.princeton.edu/rvan/acm217/ACM217.pdf>, vol. 14, 2007.
- [42] A. V. Savkin and I. R. Petersen, "Minimax optimal control of uncertain systems with structured uncertainty," *International Journal of Robust and Nonlinear Control*, vol. 5, no. 2, pp. 119–137, 1995.
- [43] S. Chen, "The robust optimal control of uncertain systems-state space method," *IEEE transactions on automatic control*, vol. 38, no. 6, pp. 951–957, 1993.
- [44] M. Grant and S. Boyd, "CVX: Matlab software for disciplined convex programming, version 2.1," <http://cvxr.com/cvx>, 2014.
- [45] —, "Graph implementations for nonsmooth convex programs," in *Recent Advances in Learning and Control*, ser. Lecture Notes in Control and Information Sciences, V. Blondel, S. Boyd, and H. Kimura, Eds. Springer-Verlag Limited, 2008, pp. 95–110, http://stanford.edu/~boyd/graph_dcp.html.